LI, H., WANG, S, ISLAM, M., BOBOBEE, E.D., ZOU, C. and FERNANDEZ, C. 2022. A novel state of charge estimation method of lithium-ion batteries based on the IWOA-AdaBoost-Elman algorithm. *International journal of energy research* [online], 46(4), pages 5134-5151. Available from: https://doi.org/10.1002/er.7505

A novel state of charge estimation method of lithium-ion batteries based on the IWOA-AdaBoost-Elman algorithm.

LI, H., WANG, S, ISLAM, M., BOBOBEE, E.D., ZOU, C. and FERNANDEZ, C.

2022

INTERNATIONAL JOURNAL OF ENERGY RESEARCH

A novel state of charge estimation method of lithium-ion batteries based on the IWOA-AdaBoost-Elman algorithm

Journal:	*International Journal of Energy Research*
Manuscript ID	ER-21-21169.R3
Wiley - Manuscript type:	Research Article
Date Submitted by the Author:	11-Nov-2021
Complete List of Authors:	li, huan Wang, Shunli; Southwest University of Science and Technology, School of Information Engineering Islam, Monirul Bobobee, Etse Dablu; Southwest University of Science and Technology Zou, Chuan-Yun Fernandez, Carlos; Robert Gordon University
Keywords:	lithium-ion battery, state of charge, Improved Whale Optimization Algorithm, AdaBoost, Elman neural network

A novel state of charge estimation method of lithium-ion batteries based on the IWOA-AdaBoost-Elman algorithm

Huan Li[a], Shun-Li Wang[a*], Monirul Islam [a], Etse Dablu Bobobee [a], Chuan-Yun Zou[a], Carlos Fernandez[b]

[a]School of Information Engineering, Southwest University of Science and Technology, Mianyang 621010, China; [b]School of Pharmacy and Life Sciences, Robert Gordon University, Aberdeen AB10-7GJ, UK.

Abstract: Lithium-ion (Li-ion) battery is a very complex nonlinear system. The data-driven state of charge (SOC) estimation method of Li-ion battery avoids complex equivalent circuit modeling and parameter identification, which can describe the nonlinearity of the battery more directly and accurately. To address the problems of low generalization ability, local miniaturization, low prediction accuracy and insufficient dynamics in the prediction process of a single feedforward neural network, an IWOA-AdaBoost-Elman algorithm-based SOC estimation method for lithium-ion batteries is proposed. The method introduces an Improved Whale Optimization Algorithm (IWOA) to continuously optimize the nonlinear weights of the Elman neural network during the iterative process. Using the AdaBoost algorithm, multiple weak IWOA-Elman predictors are recombined into one strong SOC estimator by successive iterations. The combined strong predictor has strong generalization ability, estimation accuracy and dynamic characteristics. To verify the rationality of the model, the SOC estimation is performed under dynamic operating conditions. The experimental results show that the proposed method is more accurate and stable compared with other optimization models. In addition, the proposed method can overcome the effects of different discharge multipliers, different ambient temperatures and different aging cycles on SOC estimation. Both theoretical and experimental results show that the IWOA-AdaBoost-Elman algorithm provides a new way for the SOC estimation of Li-ion batteries.

Keywords: lithium-ion battery; state of charge; Improved Whale Optimization Algorithm; AdaBoost; Elman neural network

***Corresponding author**: Shun-Li Wang. Tel: +86-15884655563. E-mail address: 497420789@qq.com.

1. Introduction

Currently, lithium-ion batteries are dominant in the EV battery market due to their high power and energy density, high voltage, extended life cycles and low self-discharge rates. Nevertheless, lithium batteries are sensitive to aging and temperature; thus, special focus is required on their working environments to avoid any physical damage, aging, and thermal runaways[1, 2]. BMS can manage a secondary battery or battery pack by protecting the battery within its safe range of operation and closely monitoring battery characteristics such as state of charge (SOC), state of health (SOH), thermal management, and battery balance state. Highly accurate battery SOC[3] values are the key to an efficient BMS, which is used to measure the remaining usable power of the battery in its current state, and some researchers use SOC to estimate SOH and remaining useful life(rul). Wang et al. [4]used the equivalent internal impedance to estimate the SOH of Li-ion batteries by considering the influences of temperature and SOC. Incremental capacity (IC) and differential voltage (DV) analysis can also be used to estimate SOH based on accurate estimation of SOC[5]. In addition, accurate SOC estimation has a very important role in battery troubleshooting, Zhang et al. [6]proposed a real-time diagnosis method for soft-short circuit(SSC) fault of series-connected lithium-ion battery pack based on the cell difference model (CDM) and low-pass filters. Yao et al. [7]proposed an intelligent fault diagnosis method for lithium battery systems based on grid search SVM, which can identify the potential fault state and classify the severity of the fault. Shang et al. [8]proposed a multi-fault diagnosis method for early battery failure prediction based on the modified sample entropy. In the operating state, the battery system works in a nonlinear state at all times. Currently, the main methods for SOC estimation are open-circuit voltage algorithm[9, 10], current integration method[11, 12], physical model method[13, 14] and data-driven method[12, 15-18]. The open-circuit voltage method is commonly used in industry to calibrate SOC, but accurate measurement of OCV takes a long time. The current integration method is used to achieve SOC estimation by integrating current over time. However, accurate initial values of SOC are difficult to obtain, while the accuracy of SOC estimation decreases with the accumulation of current measurement errors. Physical modeling methods include Kalman filter[19], sliding mode observer[20, 21], and particle filter[22, 23]. Kalman filters are widely used, including extended Kalman filter[24-26], unscented Kalman filter[27-29], and adaptive Kalman filter[30-32]. Although these methods have better robustness and estimation accuracy, it is difficult to build an accurate battery equivalent circuit model due to internal resistance and capacitance variation, and the computational cost is high. Data-driven machine learning methods such as neural networks and support vector machines[7, 33] build nonlinear relational models characterizing the external characteristics of the battery through the inputs and outputs of the battery system. Environmental disturbances such as external temperature[34, 35] and aging conditions[2, 36] can also be considered.

With the rapid development of artificial intelligence and machine learning methods, data-driven estimation methods have been widely used to estimate Li-ion battery SOC. The data-driven method can efficiently solve battery data acquisition nonlinearity and instability issues. The neural network is an important data-driven learning method based on self-organization, self-adaptation, and self-learning, which can model and simulate complex nonlinear objects and is suitable for capturing the nonlinear and dynamic characteristics of battery systems. BPNN is a representative algorithm in neural networks and has a wide range of applications in battery SOC estimation. Xuan et al.[37] has developed a SOC estimation model based on BPNN for Li-ion batteries and achieved good results. However, BP neural networks still have algorithmic drawbacks in SOC estimation, such as local miniaturization, limited prediction accuracy, and overfitting. The feedforward neural network lacks a memory mechanism and has poor dynamic adaptability. Chemali et al.[38] built a deep feedforward neural network (DFNN) to estimate the SOC under different operating conditions and different temperatures. It was pointed out that the DFNN is suitable for handling nonlinear systems of Li-ion batteries, but the training time is too long and complex processor units are required. ELM has the characteristics of fast learning speed, high stability and generalization. Lipu et al.[39] used current, voltage and temperature as input features, an ELM-based SOC estimation model was designed, but the number of suitable implied layers limits the performance of this model. Recently, many scholars are keen on using hybrid deep learning methods to optimize the accuracy of SOC estimation. Song et al.[40] applied a combination of convolutional neural network (CNN) and LSTM to estimate SOC, which proved to be a very effective but computationally intensive model for predicting nonlinear systems and solving time series problems. To a certain extent, "shallow model" based estimation methods can effectively fit nonlinearities. Still, it is difficult to effectively capture the dynamic characteristics of the battery in the time dimension of physical or electrochemical properties. However, the direct introduction of complex neural networks is computationally intensive and prone to overfitting, so more effective data-driven SOC estimation methods need to be explored. To solve these issues, this study uses an Elman neural network for SOC estimation of lithium-ion batteries. The network structure is very simple, and its topology has one more undertaking layer than the feedforward static BP neural network. The undertaking layer makes the network structure with memory function and facilitates the modeling of the dynamic system process. However, the input weights of the network and the thresholds of the hidden nodes are obtained randomly, which easily leads the network to fall into the local optimum. To solve this problem, an improved whale optimization algorithm (IWOA) is proposed in this study to optimize Elman neural network. In addition, this study uses the integrated learning AdaBoost algorithm[41, 42] to form a strong predictor by combining several IWOA-Elman predictors through a combination strategy to further improve the estimation accuracy of the model. The IWOA-AdaBoost-Elman model fully exploits the advantages of different algorithms, so that the combined strong predictor has good estimation accuracy and generalization ability, and also has dynamic characteristics. The contributions of this paper are multifaceted. Firstly, this study innovatively proposes the IWOA-AdaBoost-Elman combination model. The IWOA algorithm is proposed by improving the formulation for the problem that WOA is prone to fall into local optimum. Secondly, this study verifies that the proposed model has better robustness and higher accuracy than other models under dynamic working conditions. Besides, we discuss the SOC estimation capability of the proposed model under different multiplicity, different temperature and different aging degree.

2. Mathematical analysis

2.1. Elman neural network

Compared with the BP neural network, the Elman neural network has a three-layer (input layer, hidden layer, and output layer) structure and adds an undertaking layer. The undertaking layer serves primarily as a feedback link between the input and hidden layers. The Elman neural network can reflect the delay between input and output in time. The structure of the Elman neural network is shown in Fig. 1.

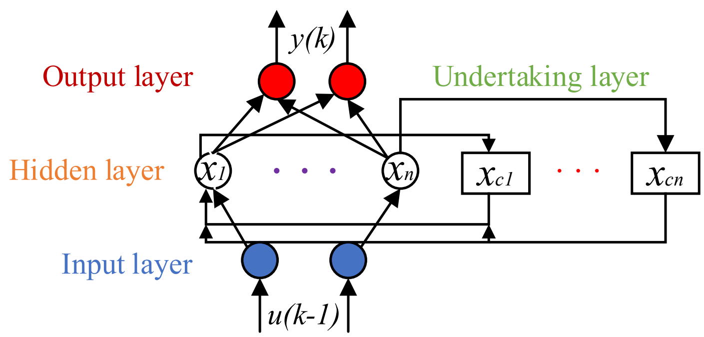

Fig. 1. The structure of the Elman neural network

Fig. 1 is the structure of the Elman neural network, which the following mathematical model can describe.

$$x(k) = f(w_1 x_c(k) + w_2 u(k-1)) \tag{1}$$

$$x_c(k) = a x_c(k-1) + x(k-1) \tag{2}$$

$$y_k = w_3 x(k) \tag{3}$$

$$f(x) = \frac{1}{1+e^{-x}} \tag{4}$$

In the above equation, w_1 is the connection weight matrix between the undertaking layer and the hidden layer, w_2 is the connection weight matrix between the input layer and the hidden layer, and w_3 is the connection weight matrix between the output layer and the hidden layer. $x(k)$ and $x_c(k)$ represent the output of the hidden layer and the undertaking layer, y_k represents the output of the output layer, and a is the self-connected feedback gain factor.

2.2. Traditional WOA algorithm

Elman neural network has a strong dynamic memory and time-varying capability. Because it randomly selects the initial value and threshold value and uses the gradient descent method to optimize. Its network learning speed is slow, and the prediction accuracy is relatively low. Therefore, this study uses the IWOA algorithm to optimize the initial weights and thresholds of the Elman neural network.

The WOA algorithm is a new type of population intelligence optimization algorithm proposed by Seyedali Mirjalili and others in 2016, a heuristic algorithm that simulates the social behavior of humpback whales. The algorithm includes three main stages: randomly searching for food, encircling predation, and bubble predation. The algorithm flowchart is shown in Fig. 2.

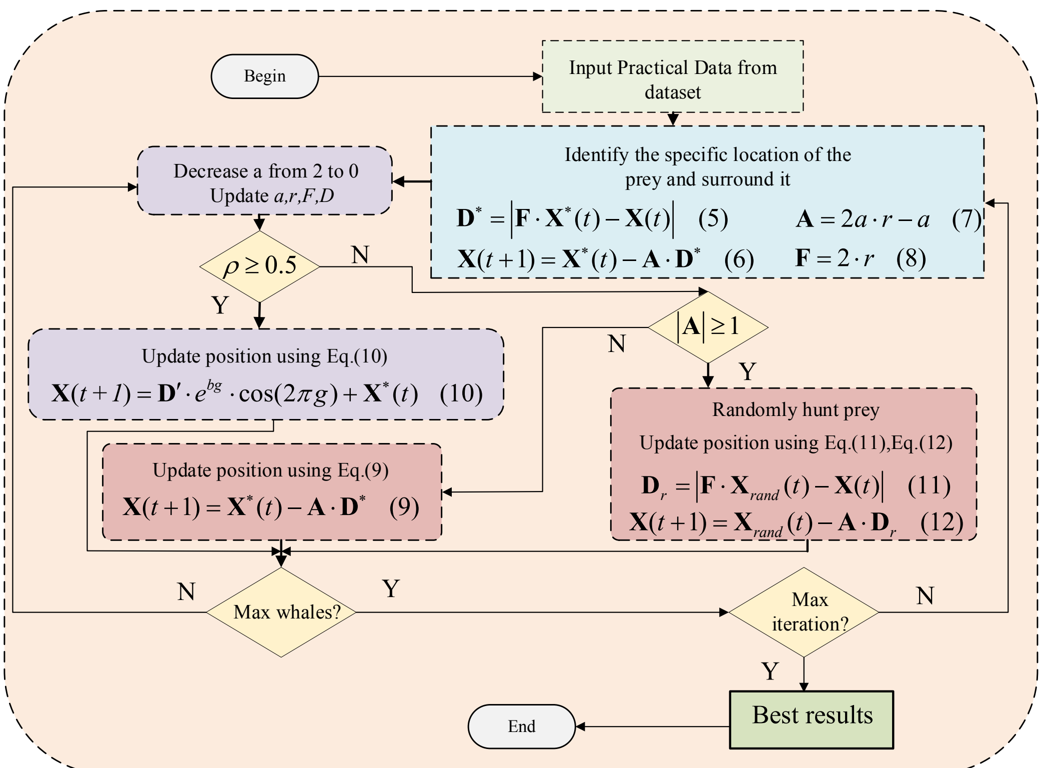

Fig. 2. The flowchart of the WOA algorithm

The equation shown in Fig. 2, t represents the number of current iterations; **A** and **F** are coefficient vectors; r is a random vector on the range [0,1]. The b denotes the constant of the logarithmic helix, g is a random number in

[-1,1], and p is the probability of randomness.

2.3. IWOA- Elman algorithm

The traditional WOA algorithm[43, 44] is an effective optimization technique. However, the algorithm converges very quickly at the beginning of the evolution process, although it is easy to fall into a local search. The specific reason is that WOA uses parameter A to adjust the balance between the development phase and the conversion of the exploration phase. Use Eq. (12) and Eq. (5) to select the development phase or the exploration phase, but the probability of selecting these two equations is not equal. Further calculation of Eq. (7) can be rewritten as Eq. (13)

$$\begin{aligned}\mathbf{A} &= 2\cdot a\cdot r-a \\ &=[2\cdot r-1]\cdot a \\ &=\mu\cdot a\end{aligned} \tag{13}$$

In Eq. (13), μ is a uniformly distributed random real number on the interval [-1,1]. The parameter a decreases linearly from 2 to 0 in the iterative process. Therefore, when Eq. (5) is executed in the second half of the optimization process, Eq. (14) always holds. In the first half of the optimization process, the probability of executing Eq. (5) can be calculated as Eq. (15).

$$|\mathbf{A}|=|\mu\cdot a|<1 \tag{14}$$

$$\begin{aligned}&\rho(|\mathrm{A}|<1)=\rho(|\mu\cdot a|<1) \\ &=0.5+\int_{0.5}^{1}\int_{1}^{1/\mu} dad\mu \\ &=0.5+\int_{0.5}^{1}(\frac{1}{\mu}-1)d\mu \\ &=0.5+(\ln\mu-\mu)|_{0.5}^{1} \\ &=\ln 2\approx 0.693\end{aligned} \tag{15}$$

It can be seen from Eq. (15) that even in the first half of the evolutionary process, the probability of Eq. (5) being selected is relatively large. In fact, under the premise of ρ<0.5 in the whole optimization process, the total probability of executing Eq. (5) is $\rho(|\mathbf{A}|<1)$=0.5+0.5×ln2≈0.847. Therefore, the dominance of Eq. (5) in the optimization algorithm is higher than that of Eq. (12). On the other hand, in the early stage of the optimization algorithm, the value **A** is relatively large, providing a large disturbance to help the WOA algorithm jump out of the local optimum. However, as the optimization process progresses, this disturbance will rapidly decrease, which is not conducive to the exploration phase.

Based on the above analysis, it is obvious that WOA places an undue emphasis on the development phase, which tends to lead to premature convergence to a local optimum. An improved WOA (IWOA) is presented to address the drawbacks of the original WOA while also efficiently balancing the development and exploration phases. By improving the WOA search method, the IWOA algorithm is globally optimal, fast and stable. An improved model based on IWOA optimized Elman network is proposed, and the structure of the model is shown in Fig. 3.

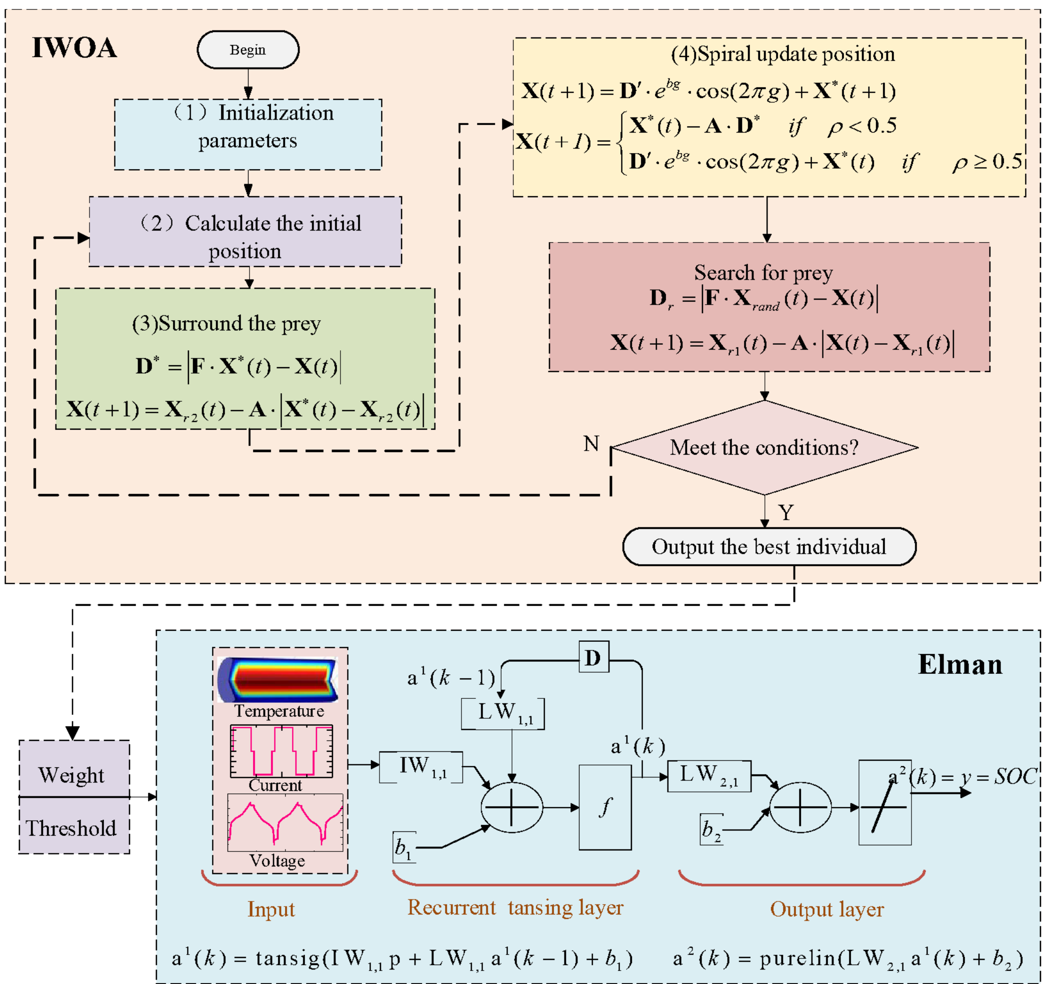

Fig. 3. IWOA-Elman model

As shown in Fig. 3, Eq. (12) and (5) in the original WOA algorithm are replaced by Eq. (16) and (17) in the IWOA model, respectively.

$$\mathbf{X}(t+1) = \mathbf{X}_{r1}(t) - \mathbf{A} \cdot \left|\mathbf{X}(t) - \mathbf{X}_{r1}(t)\right| \tag{16}$$

$$\mathbf{X}(t+1) = \mathbf{X}_{r2}(t) - \mathbf{A} \cdot \left|\mathbf{X}^{*}(t) - \mathbf{X}_{r2}(t)\right| \tag{17}$$

The *r1* and *r2* in Eq. (16) and Eq. (17) denote two different random individuals. The core idea of the IWOA algorithm proposed in this study is based on three considerations. First, the symmetric perturbation of $\mathbf{X}_{r2}(t)$ using $\mathbf{A} \cdot \left|\mathbf{X}^{*}(t) - \mathbf{X}_{r2}(t)\right|$ in Eq. (17) can enhance the optimized population variability. Second, although the dominance of Eq. (17) is still higher than that of Eq. (16), both equations use a random individual to update the current individual, which can enhance the exploration based on the existing development stage, thus making a good balance between the two. Third, dropping the coefficient F promotes robustness by ensuring the consistency of the distance between two individuals. IWOA retains the basic structure of the original WOA and does not introduce additional parameters or other complex search operators that require tuning. As a result, the optimization times of the two algorithms are essentially the same.

2.4. IWOA-Elman-AdaBoost

The AdaBoost algorithm is a typical integration algorithm that will recalculate the classifier's classification error rate after each iteration. To improve the classification accuracy of the iterations, the initial weights of the training samples with high error rates in the previous iteration are increased in the next iteration. Finally, multiple weak classifiers are organically combined to form a strong classifier to achieve an overall improvement in recognition accuracy.

The Elman neural network optimized by the IWOA algorithm has the advantages of fast convergence and not easy to fall into local minima, while the AdaBoost algorithm has the advantages of serial integration learning, which becomes a strong predictor by combining the interdependencies of weak predictors and according to certain weights. In this study, the IWOA-AdaBoost-Elman based SOC estimation algorithm is proposed. The core idea is to transform the data layer fusion problem into the decision layer fusion problem by using the integration learning theory. The structure of this model is shown in Fig. 4.

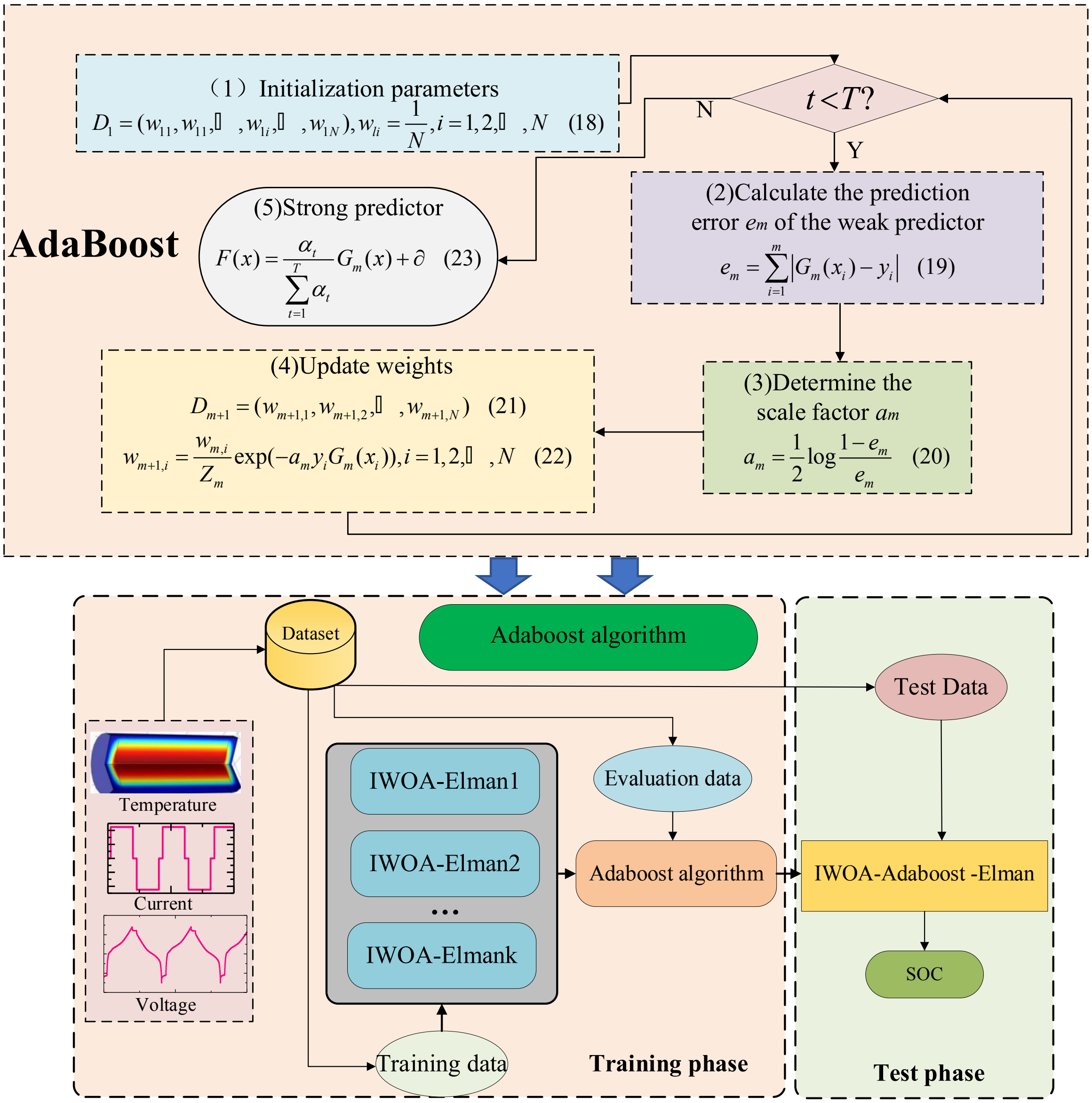

Fig. 4. Algorithm implementation steps of AdaBoost

As the algorithm steps are shown in Fig. 4, the sample data are divided into the training set, test set, and input training set. The training sample weights need to be initialized, D_1 is the set of weights of the dataset, N represents the number of samples, and w represents the initial weight of each sample. Using the AdaBoost algorithm, some weak predictors (IWOA-Elman) are formed into strong predictors and utilized to predict lithium-ion battery SOC.

2.5. Algorithm evaluation metrics

To evaluate the established SOC estimation model and compare the predicted data with the actual data, three statistics were selected in this study: mean absolute error (MAE), mean absolute percentage error (MAPE), and root mean square error (RMSE). The specific calculation expressions for each type of error are as follows.

$$\mathrm{RMSE} = \sqrt{\left[\frac{1}{N}\sum_{i=1}^{N}\left|Y_i - \hat{Y}_i\right|^2\right]} \tag{24}$$

$$\mathrm{MAE} = \frac{1}{N}\sum_{i=1}^{N}\left|Y_i - \hat{Y}_i\right| \tag{25}$$

$$\mathrm{MAPE} = \frac{1}{N}\sum_{i=1}^{N}\left|\frac{Y_i - \hat{Y}_i}{Y_i}\right| \tag{26}$$

Y denotes the true SOC value, $\hat{Y}$ is the predicted SOC value, and N represents the number of samples.

3. Experimental analysis

3.1. Test equipment and procedures

The research materials are ternary lithium-ion batteries with a rated capacity of 70Ah and 18650 lithium-ion cobalt-acid batteries with a rated capacity of 2Ah. The BTS200-100-104 battery testing and temperature control equipment are used in this work to construct an experimental platform and collect important experimental data. The experimental battery platform constructed is shown in Fig. 5.

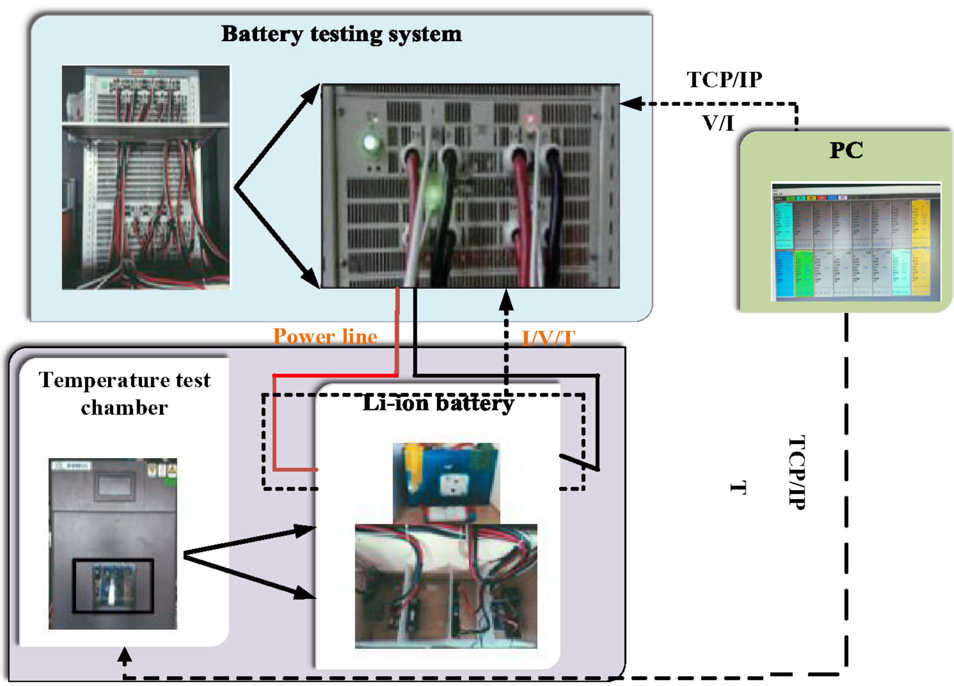

Fig. 5. The experiments platform construction

3.2. *Dynamic working condition test*

In the actual use environment of Li-ion batteries, the operating conditions are complex and variable. To verify the stability of the improved algorithm for SOC estimation under complex operating condition and the strong tracking, dynamic operating conditions experiments of DST and BBDST are conducted on Li-ion batteries at an ambient temperature of 25°C. This study uses the DST working condition as the training set, a complex working condition evolved from the US federal city operating condition and contains the process of continuous charging and discharging of the lithium battery. BBDST working condition is used as the test set, which includes 19 working steps such as starting, coasting, accelerating, braking, and rapid acceleration of the pure electric bus. It can better restore the real working condition of a lithium battery. The data set is shown in Fig. 6.

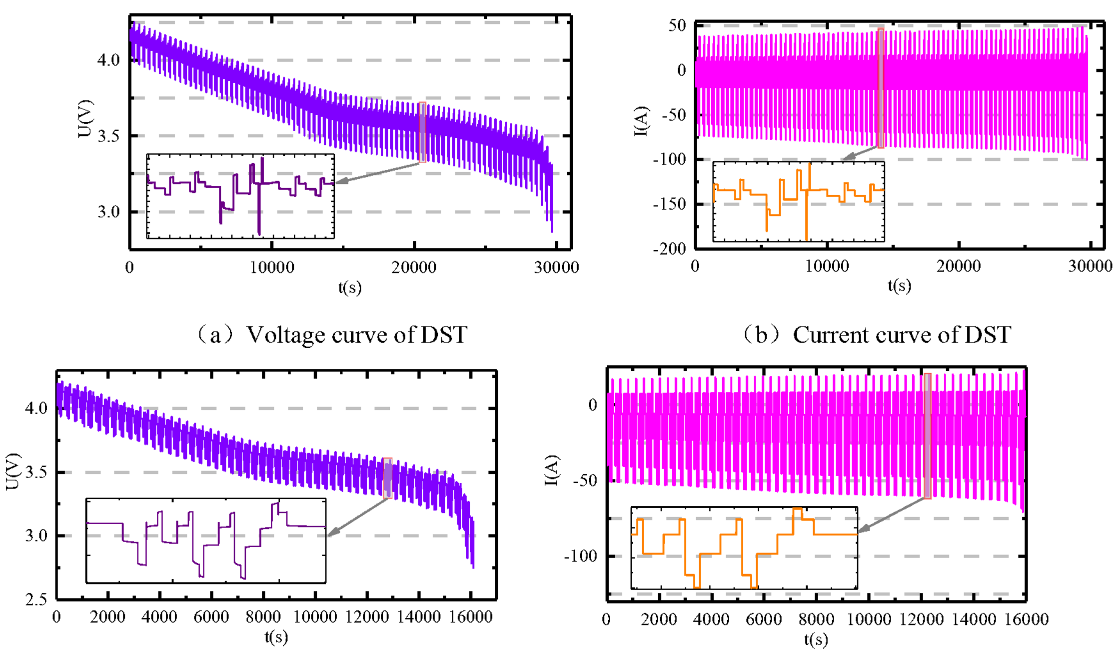

（a） Voltage curve of DST

（b） Current curve of DST

（c） Voltage curve of BBDST

（d） Current curve of BBDST

Fig. 6. Data sets for dynamic working conditions

In order to verify the effectiveness of the improved algorithm, the simulation effects of Elman neural network, IWOA-Elman neural network and IWOA-Elman-Adaboost model were tested separately with the same parameters of the network model. Besides, the dynamic responsiveness of the IWOA-Elman-Adaboost model with different initial values is tested. In this experiment, all neural networks are structured with a single hidden layer of 8 nodes in order to satisfy the fast nature of the algorithm. The simulation results and the error analysis are shown in Fig. 7.

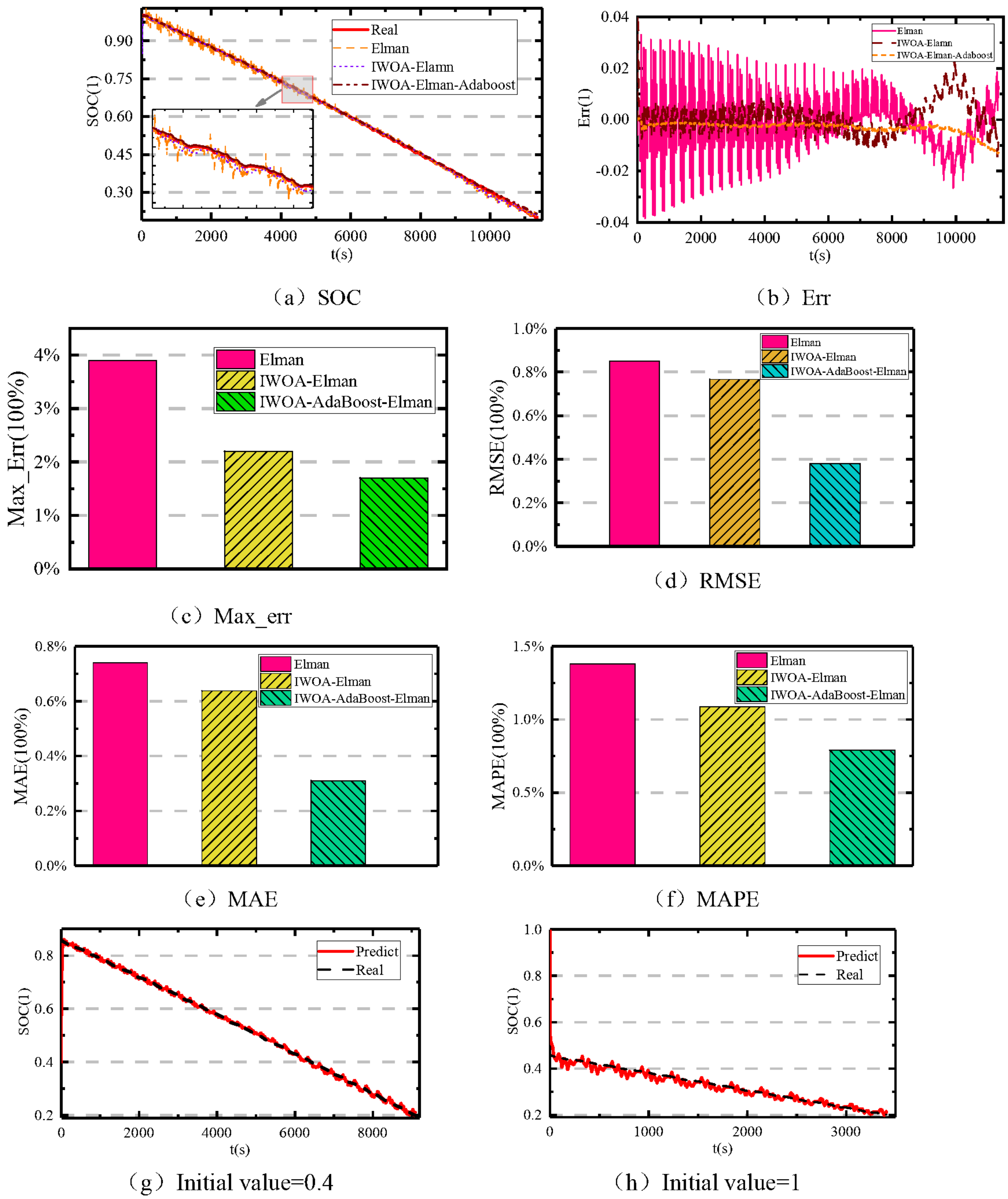

Fig. 7. Simulation of SOC estimation under dynamic working conditions

As shown in Fig. 7. From (a) and (b), it can be seen that the IWOA-optimized Elman neural network performs significantly better than the Elman model alone under dynamic operating conditions. With further optimization by Adaboost, the SOC estimation curve of the IWOA-Elman-Adaboost model always follows the reference curve.

The error fluctuates in a narrow range throughout the simulation and is smaller than the other two models, proving that the IWOA-Elman-Adaboost model has strong robustness. To further compare the SOC estimation results visually, the maximum absolute errors, RMSE, MAE, and MAPE of each model are plotted in the histograms as shown in (c), (d), (e), and (f). The maximum error of the Elman neural network is 3.9%, and its RMSE, MAE, and MAPE are 0.85%, 0.74%, and 1.38%, respectively. The maximum error of the Elman model after IWOA optimization was reduced to 2.2%, and its RMSE, MAE, and MAPE decreased to 0.77%, 0.64%, and 1.08%, respectively. IWOA improved the accuracy of Elman's SOC estimation. The Elman-Adaboost model further optimized by Adaboost has higher accuracy, it reduces the maximum error to 1.7%, and its RMSE, MAE, and MAPE decrease to 0.38%, 0.31%, and 0.79%, respectively, compared with the Elman and IWOA-Elman models, the accuracy is improved by 56.4% and 22.7%. Figures (g) and (h) show that the IWOA-Elman-Adaboost model still has high accuracy and fast responsiveness in the case of invalid initial values.

The IWOA-Adaboost-Elman model has a great advantage over the Elman and IWOA-Elman models. To further demonstrate the superiority of this model, the effects of WOA, GA and MAE optimization of the Elman model are tested and compared under the same dataset, respectively. The simulation test results of different optimization algorithms are shown in Fig. 8.

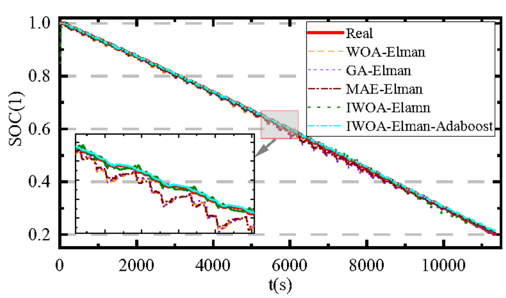

（a） SOC

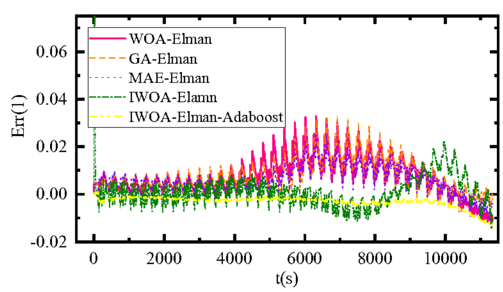

（b） Err

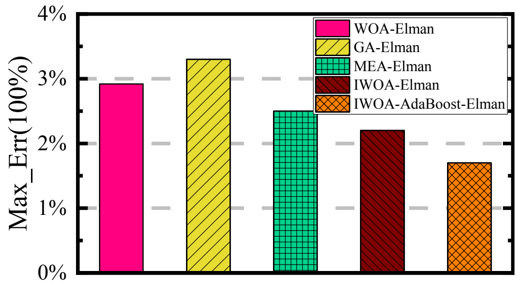

（c）Max_err

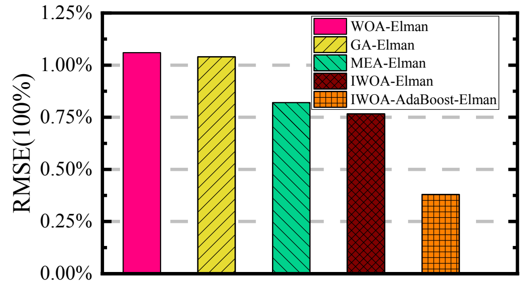

（d）RMSE

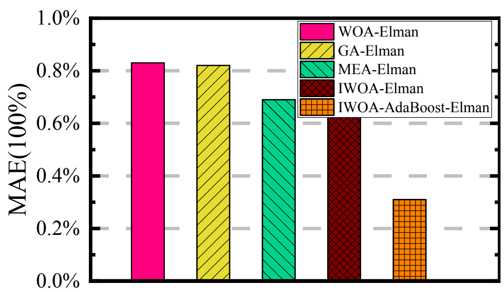

（e）MAE

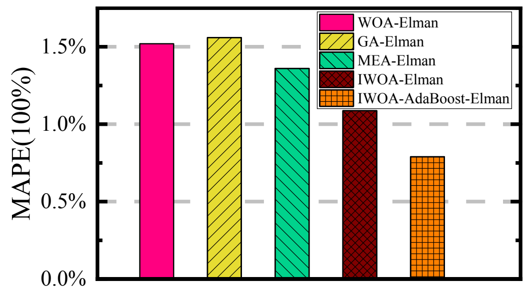

（f）MAPE

Fig. 8. Simulation test results of various optimization algorithms under dynamic working conditions

As shown in Fig. 8, (a) and (b) illustrate the SOC simulation results and their errors. From the figures, it can be seen that the IWOA-Elman-Adaboost model follows the real value steadily in all phases of the operating conditions, and the errors remain in a small range. In contrast, the other optimization models show some degree of instability and tend to diverge. From the histograms of (c), (d), (e), and (f), it can be seen that the IWOA-Elman-Adaboost model has a significant advantage over the other algorithms in terms of all indicators. This further confirms the superiority of the method for SOC estimation.

3.3. SOC estimation at different discharge currents

Parameters such as capacity, energy and open-circuit voltage of Li-ion batteries are crucial indicators of their performance and key parameters affecting SOC estimation. In this study, a ternary lithium battery with a rated capacity of 70AH will be used as the research object, and constant current discharge experiments with different discharge currents will be carried out at an ambient temperature of 25°C. The changes of key parameters under different discharge currents are shown in Fig. 9.

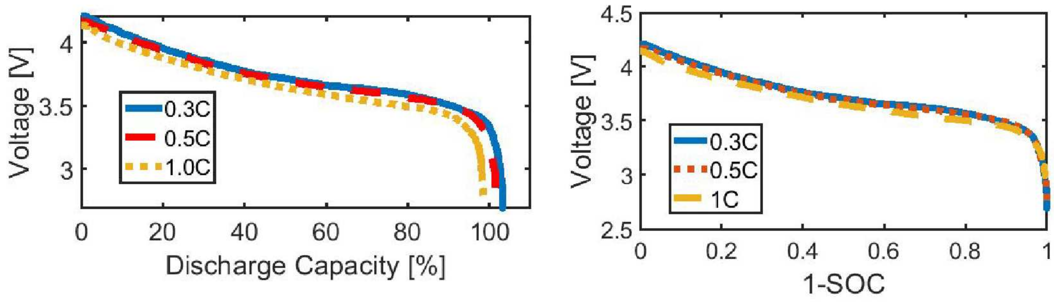

（a）Relationship between open-circuit voltage and capacity （b）Relationship between open-circuit voltage and SOC

Fig. 9. The changes of key parameters under different discharge currents

As shown in Figure 9, (a) points out that the releasable capacity of the battery is negatively correlated with the magnitude of the discharge current. From (b), it can be seen that the battery discharge current influences the open-circuit voltage of the battery in the late stage of discharge, and the higher the discharge multiplier, the faster the open-circuit voltage decreases.

Considering that the key parameters change under different discharge currents, which affects the SOC estimation, to verify that the proposed model can overcome the effects caused by different discharge currents on SOC estimation, the 0.5C discharge data is used as the training set and validated by the data under 0.3C and 1C. In this experiment, the IWOA and Adaboost parameters of each model are the same, and they all adopt the single hidden layer structure. FNN, BP and RBF all have 12 hidden layer nodes, and Elman has 8 hidden layer nodes. The simulation results are shown in Fig. 10.

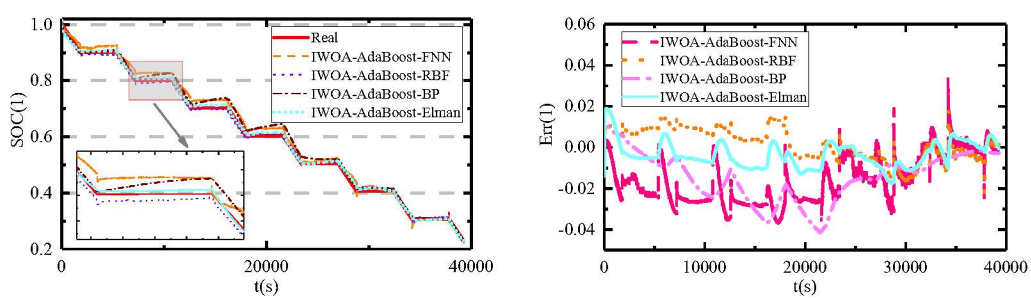

（a1）SOC （a2）Err

(a) Simulation test results under 0.3C discharge

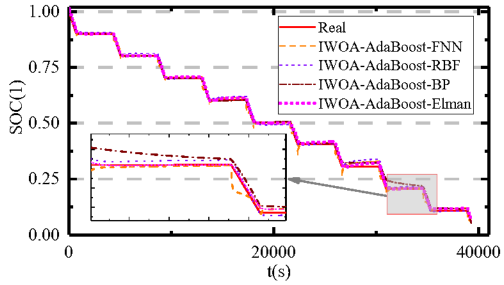

(b1) SOC

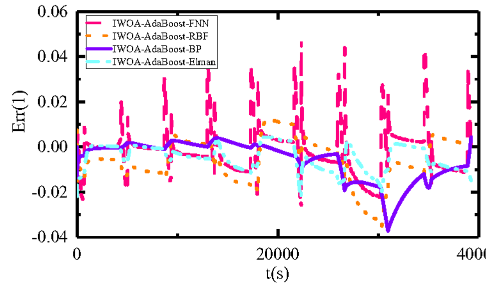

(b2) Err

(b) Simulation test results under 0.5C discharge

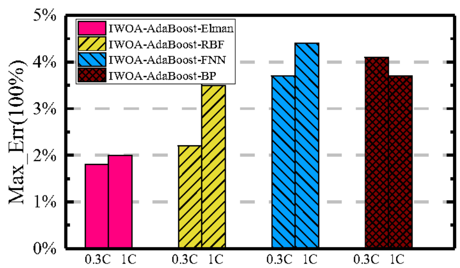

(c) Max_err

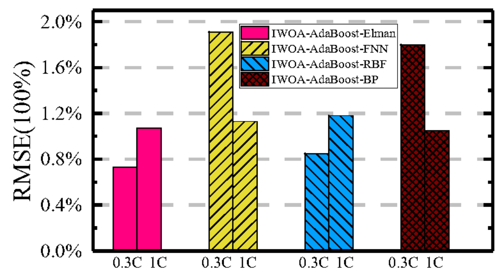

(d) RMSE

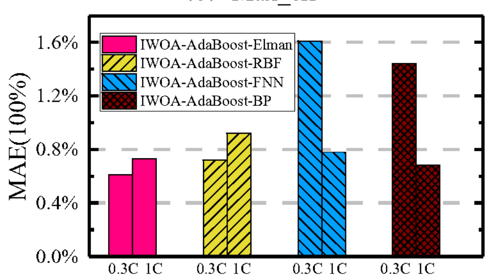

(e) MAE

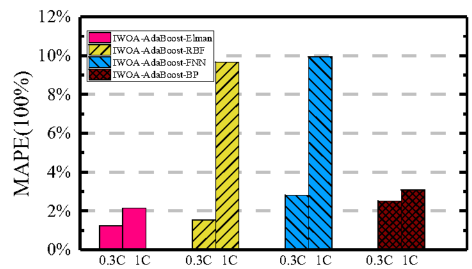

(f) MAPE

Fig. 10. Simulation test results at different discharge currents

As shown in Figure 10, it is clear from (a) and (b) that the IWOA-Adaboost-Elman model maintains good convergence at both high and low discharge currents, with smaller errors and outstanding robustness compared to other models. From (c), (d), (e), and (f), it can be seen that the maximum error of IWOA-Adaboost-Elman under both high and low discharge rates is less than 2%, which is much lower than other models. Its three indexes of RMSE, MAE, and MAPE are significantly better than other models. This proves that IWOA-Adaboost-Elman has higher accuracy than other models and confirms that the proposed method can overcome the effect of different discharge currents on SOC estimation.

3.4. SOC estimation at different temperatures

The total capacity of a Li-ion battery is used as one of the crucial variables for estimating the battery SOC. It is closely related to the operating environment temperature, which is often considered a constant value in the SOC estimation algorithm, thus affecting the SOC estimation accuracy under different environmental temperatures. Considering the influence of temperature on the characteristic parameters of Li-ion battery capacity, dynamic working condition experiments are conducted at different temperatures, respectively. The relationship between the key parameters of Li-ion battery SOC estimation and temperature is shown in Fig. 11.

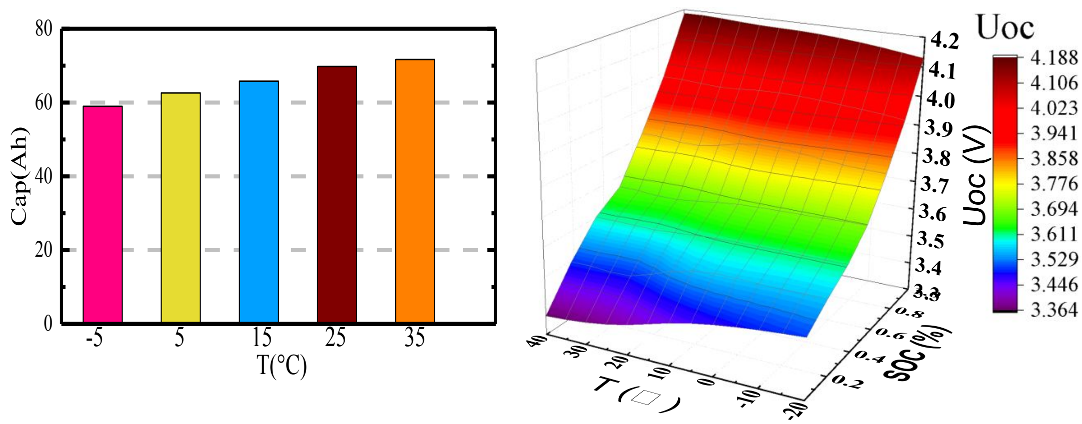

（a）Capacity variation at different temperatures

（b）SOC and open-circuit voltage versus temperature

Fig. 11. The changes of key parameters under different temperatures

As shown in Fig. 11, (a) reveals that the lithium battery capacity increases with the rises of temperature. When the temperature increases, it accelerates the occurrence of internal side reactions in Li-ion batteries, and when the temperature decreases, it causes the deposition of active lithium on the electrode surface. (b) describes the relationship between the variation of SOC and open-circuit voltage of Li-ion battery at different temperatures. From the figure, it can be seen that when the value of SOC is between 0.4 and 1, the difference of the corresponding open-circuit voltage under the same SOC value is very small, and only when the SOC value is between 0 and 0.4, there is a large difference in the open-circuit voltage. To demonstrate that the proposed method can overcome the influence of ambient temperature on the accuracy of SOC estimation, the data collected at an ambient temperature of 25°C is used as the training set and the data collected at other temperatures is used as the test set. In this experiment, the IWOA and Adaboost parameters of each model are consistent. Through several experimental comparisons, FNN, BP and RBF choose the structure of 10 nodes each in the double hidden layer. Elman uses the structure of 12 nodes in the single hidden layer. The simulation test results are shown in Fig. 12.

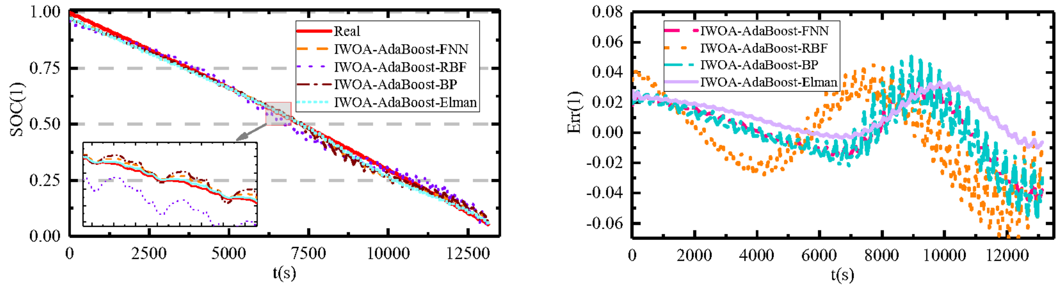

（a1） SOC （a2） Err

(a) SOC estimation results at -5°C

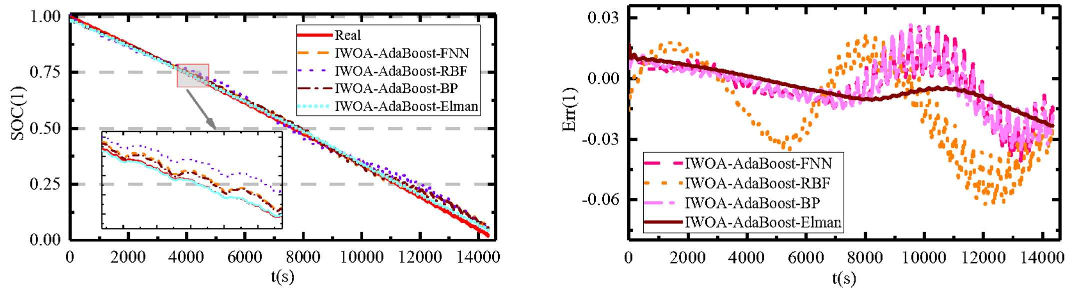

（b1） SOC （b2） Err

(b) SOC estimation results at 5°C

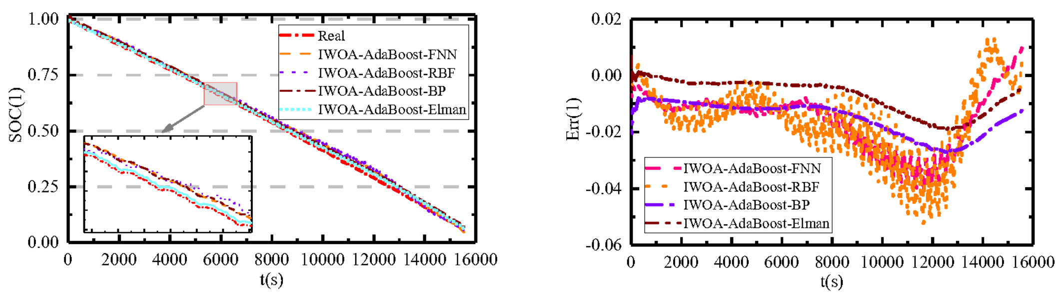

（c1） SOC （c2） Err

(c) SOC estimation results at 15°C

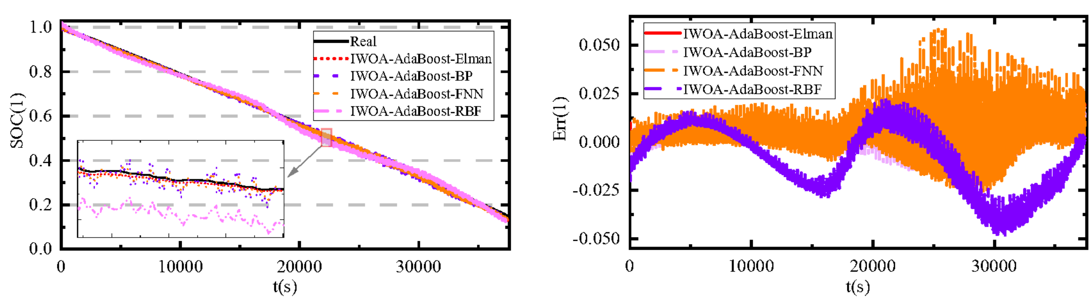

（d1） SOC （d2） Err

(d) SOC estimation results at 35°C

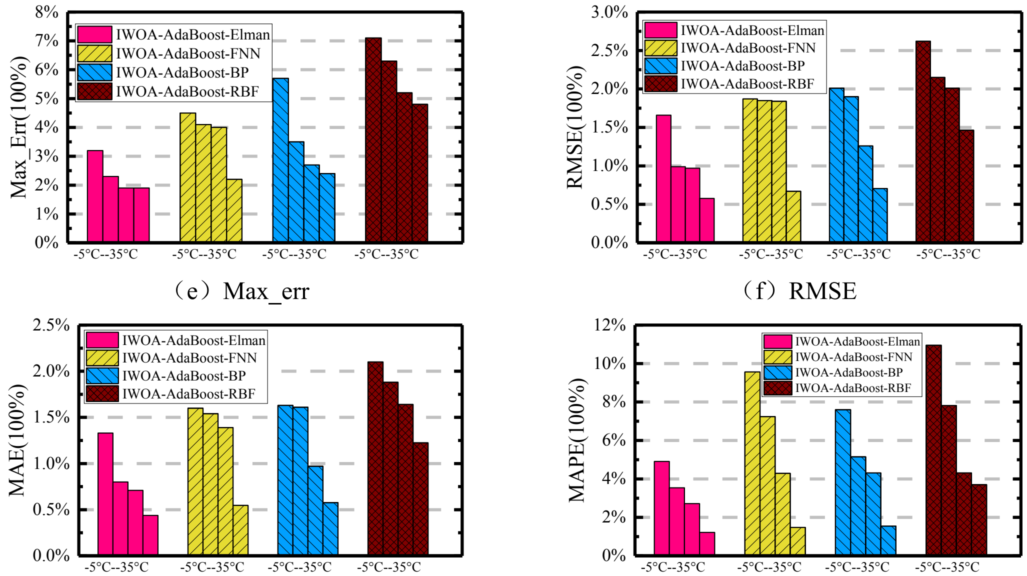

（e）Max_err （f）RMSE

（g）MAE （h）MAPE

Fig. 12. Simulation results of SOC estimation at different temperatures

As shown in Fig. 12, the IWOA-Adaboost-Elman model can follow the change of the reference value smoothly, as seen in figures (a), (b), (c), and (d). The model has good convergence and can still respond quickly to the change of the reference value under low-temperature conditions. Figures (e), (f), (g), and (h) depict more visually the error metrics of the different models. From the figures, it can be seen that the maximum absolute error of IWOA-Adaboost-Elman is less than 3.5% for both low and high-temperature conditions, which is much lower than that of other models. For other error indicators, the proposed method has more obvious advantages. The IWOA-Adaboost-Elman model's accuracy for estimating SOC under temperature variation is verified. It is further demonstrated that the model can overcome the influence of ambient temperature variation on SOC estimation.

3.5. SOC estimation under different states of health

In practical applications, as the battery ages, the battery SOC estimation error gradually increases, up to 20% to 30%. Considering the influence of battery aging on the accuracy of SOC estimation, this study will take a lithium battery (model 18650) with a rated capacity of 2Ah and conduct a cyclic aging test at an ambient temperature of 25°C. The changes of characteristic parameters under different states of health(SOHs) are shown in Fig. 13.

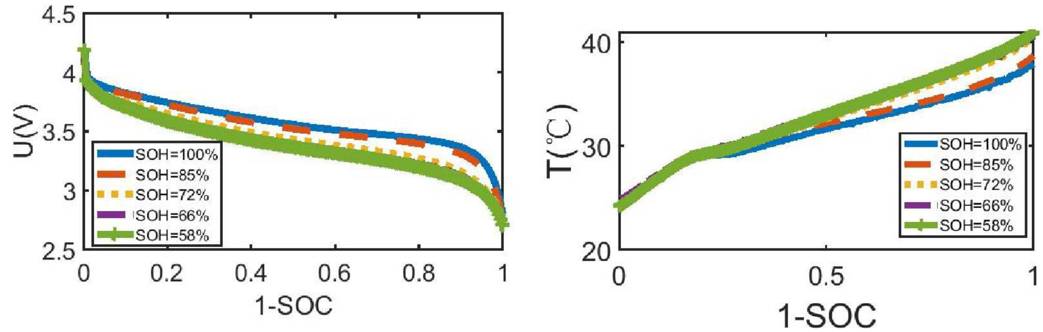

（a）Relationship between open-circuit voltage and SOC （b）Relationship between temperature and SOC

Fig. 13. The changes of key parameters under different SOHs

As shown in Fig. 13, it can be concluded from (a) that the UOC gradually decreases with the decrease of the battery's SOH at the same SOC. This illustrates that as the number of battery charge and discharge cycles increases, the rate of change of battery voltage changes and the amount of discharged power gradually decrease. (b) describes that the battery heats up faster as the battery SOH decreases at the same ambient temperature. From the above analysis, it can be obtained that the characteristic parameters of SOC estimation change significantly with the increase of battery aging. To verify whether the IWOA-Adaboost-Elman model can adapt itself to the effect of the aging degree, the unaged data will be used as the training set and the data under different aging degrees as the test set. In this experiment, the IWOA and Adaboost parameters of each model are consistent. All neural networks use a double hidden layer structure, and the number of nodes of Elman neural network is smaller compared to other neural networks. The simulation results are shown in Fig. 14.

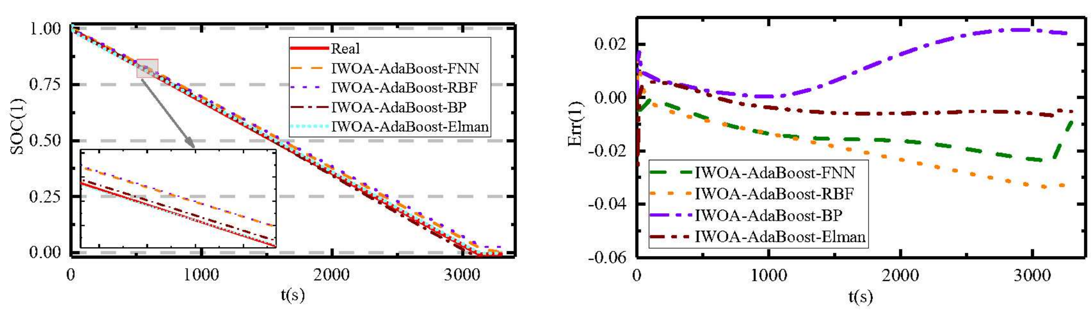

(a1) SOC (a2) Err

(a) SOC estimation results at SOH=85%

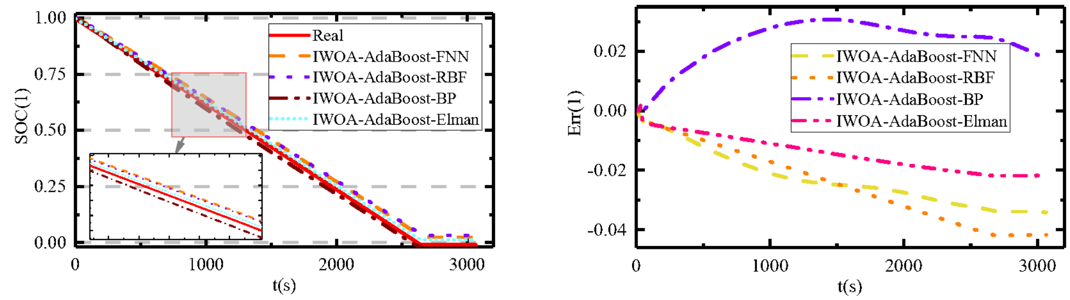

(b1) SOC (b2) Err

(b) SOC estimation results at SOH=72%

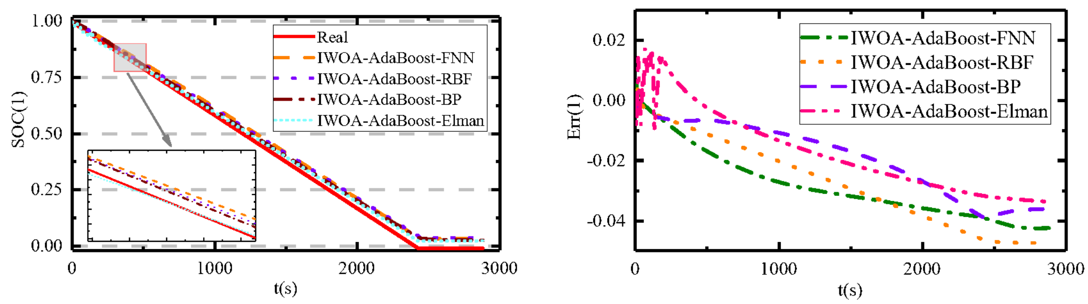

(c1) SOC (c2) Err

(c) SOC estimation results at SOH=66%

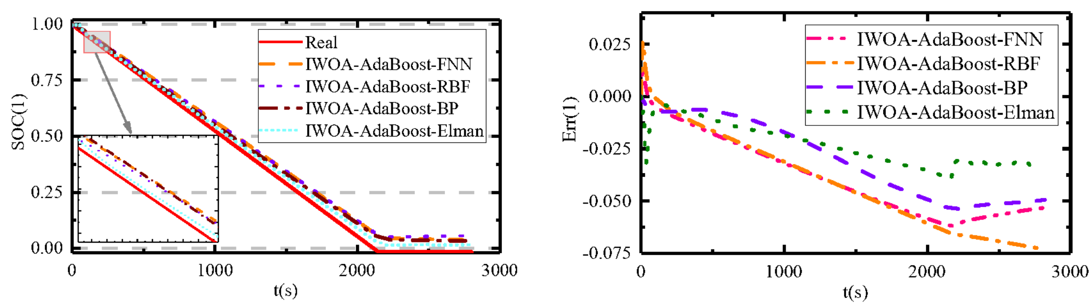

(d1) SOC (d2) Err

(d) SOC estimation results at SOH=58%

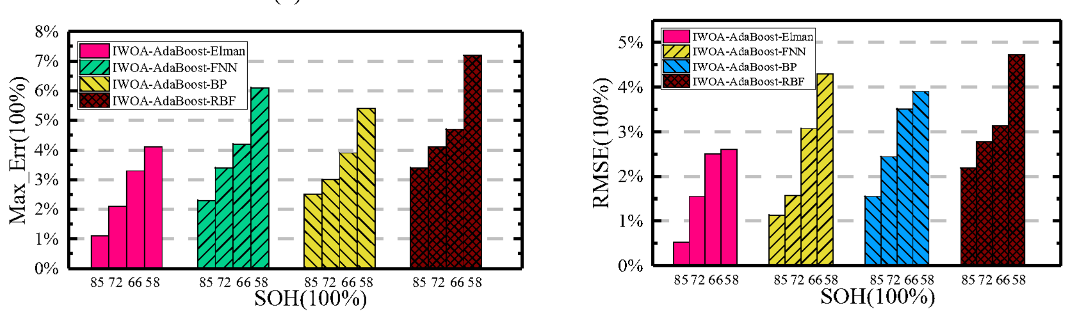

(e) max_err (f) RMSE

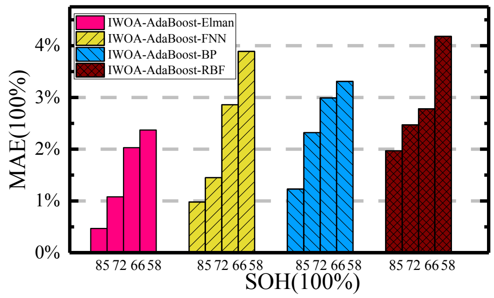

(g) MAE

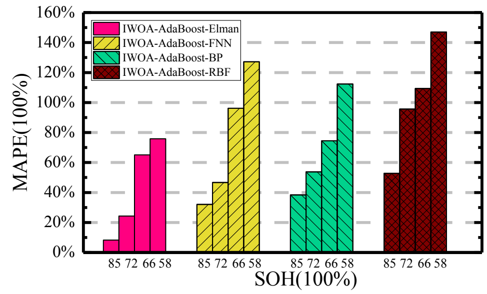

(h) MAPE

Fig. 14. SOC estimation results under different SOH

As shown in Fig. 14, it is clear from (a), (b), (c), and (d) that the IWOA-Adaboost-Elman model has higher accuracy and robustness compared to the other models at each aging stage. Figures (e), (f), (g), and (h) depict more visually the error metrics of the different models. The maximum absolute error of the IWOA-Adaboost-Elman model is 1.1% when the SOH of the battery is 85%, and the RMSE, MAE and MAPE of this model are 0.53%, 0.47% and 8.2%, respectively. After further aging, when SOH is 72%, the accuracy of SOC estimation decreases and the maximum absolute error increases to 2.1%, and all other error indicators increase. The SOC accuracy decreases further when the cell is deeply cycled, with a maximum absolute error of 4.1% when SOH drops to 58%, and RMSE and MAE reach 2.6% and 2.4%, respectively. However, the maximum absolute error of the proposed method remains below 4.5% for all aging cycles. In addition, all error metrics are significantly better than other models. It can be seen that the IWOA-Adaboost-Elman model can well address the effects of different degrees of aging on the SOC estimation of Li-ion batteries.

4. Conclusions

In this study, the IWOA-AdaBoost-Elman prediction model is proposed. We modified the search function based on the original WOA model to solve the problem of balancing local and global search in the optimization model. In addition, we innovatively use the AdaBoost algorithm to combine several weak IWOA-Elman predictors into one strong predictor, which further improves the prediction accuracy.

Experimental results show that the improved WOA improves the accuracy of Elman's SOC estimation under dynamic operating conditions. However, the IWOA-Elman-Adaboost model has higher accuracy, 56.4% and 22.7% higher than the Elman and IWOA-Elman models, respectively. Similarly, the IWOA-Elman-Adaboost model has more significant advantages over the WOA, GA and MAE optimized Elman models under the same dynamic conditions. In studying the effect of different discharge multiples on SOC estimation, we found that important parameters of SOC estimation changed at different discharge multiples. However, the IWOA-Elman-Adaboost model can still show a better advantage. It is worth noting that the combined model proposed in this study has strong generalization capability, prediction accuracy and dynamic characteristics. Despite the significant changes in the operational performance and internal properties of Li-ion batteries, the IWOA-Elman-Adaboost model can still maintain good accuracy and adaptability under various ambient temperatures and aging cycles.

In contrast to traditional estimation methods based on equivalent circuit models, this method is completely data-driven and is not limited by cell materials or models. Therefore, it can be easily applied to different types and scenarios of battery management systems. Future work will explore the SOC estimate under the fusion of multiple operating conditions, and should also consider the influence factors such as measurement noise under the battery SOC estimation in practice.

Nomenclature

The symbols used in this research can be described as shown in Tab.1.

Tab.1 List of symbols

Symbol	Description	Symbol	Description
SOC	State of Charge	ELM	Extreme Learning Machine
WOA	Whale Optimization Algorithm	CNN	Convolutional Neural Network
BPNN	Backpropagation Neural Network	LSTM	Long-Short Term Memory
OCV	Open Circuit Voltage	DST	Dynamic Stress Test
EKF	Extended Kalman Filter	BBDST	Beijing buses dynamic stress test

DFNN	Deep Feedforward Neural Network	SOH	State of Health
w_1	the connection weight matrix between the undertaking layer and the hidden layer	w_2	the connection weight matrix between the input layer and the hidden layer
w_3	the connection weight matrix between the output layer and the hidden layer	$x_c(k)$	the output of the undertaking layer
$x(k)$	the output of the output layer	a	the self-connected feedback gain factor
A,**F**	coefficient vectors	r	a random vector on the range [0,1]
b	the constant of the logarithmic helix	g	a random number in [-1,1]
p	the probability of randomness	μ	a uniformly distributed random real number on the interval [-1,1]
Y	the true SOC value	$\hat{Y}$	the predicted SOC value
rul	remaining useful life	IC	Incremental capacity
DV	differential voltage	SSC	soft-short circuit
CDM	cell difference model		

References

1. Aaldering, L.J., J. Leker, and C.H. Song, *Analysis of technological knowledge stock and prediction of its future development potential: The case of lithium-ion batteries.* Journal of Cleaner Production, 2019. **223.**

2. Xiong, R., et al., *Lithium-ion battery aging mechanisms and diagnosis method for automotive applications: Recent advances and perspectives.* Renewable & Sustainable Energy Reviews, 2020. **131**.

3. Qiu, X.H., W.X. Wu, and S.F. Wang, *Remaining useful life prediction of lithium-ion battery based on improved cuckoo search particle filter and a novel state of charge estimation method.* Journal of Power Sources, 2020. **450**.

4. Wang, X.Y., X.Z. Wei, and H.F. Dai, *Estimation of state of health of lithium-ion batteries based on charge transfer resistance considering different temperature and state of charge.* Journal of Energy Storage, 2019. **21**

5. Li, Y., et al., *Data-driven health estimation and lifetime prediction of lithium-ion batteries: A review.* Renewable & Sustainable Energy Reviews, 2019. **113**.

6. Zhang, Z.D., et al., *Real-time diagnosis of micro-short circuit for Li-ion batteries utilizing low-pass filters.* Energy, 2019. **166.**

7. Yao, L., et al., *An Intelligent Fault Diagnosis Method for Lithium Battery Systems Based on Grid Search Support Vector Machine.* Energy, 2021. **214**.

8. Shang, Y.L., et al., *A multi-fault diagnosis method based on modified Sample Entropy for lithium-ion battery strings.* Journal of Power Sources, 2020. **446**.

9. Tian, J.P., et al., *Electrode ageing estimation and open circuit voltage reconstruction*

for lithium ion batteries. Energy Storage Materials, 2021. **37**

10. Pan, B., et al., *Aging mechanism diagnosis of lithium ion battery by open circuit voltage analysis.* Electrochimica Acta, 2020. **362**.

11. Shen, D.X., et al., *A novel online method for predicting the remaining useful life of lithium-ion batteries considering random variable discharge current.* Energy, 2021. **218**.

12. Xu, T.T., Z. Peng, and L.F. Wu, *A novel data-driven method for predicting the circulating capacity of lithium-ion battery under random variable current.* Energy, 2021. **218**.

13. Sommerville, R., et al., *A review of physical processes used in the safe recycling of lithium ion batteries.* Sustainable Materials and Technologies, 2020. **25**.

14. Zhu, G.B., et al., *Correlation between the physical parameters and the electrochemical performance of a silicon anode in lithium-ion batteries.* Journal of Materiomics, 2019. **5**(2).

15. Lipu, M.S.H., et al., *Data-driven state of charge estimation of lithium-ion batteries: Algorithms, implementation factors, limitations and future trends.* Journal of Cleaner Production, 2020. **277**.

16. Zhang, S.Z., et al., *A data-driven coulomb counting method for state of charge calibration and estimation of lithium-ion battery.* Sustainable Energy Technologies and Assessments, 2020. **40**.

17. Song, Y.C., et al., *A hybrid statistical data-driven method for on-line joint state estimation of lithium-ion batteries.* Applied Energy, 2020. **261**.

18. Deng, Z.W., et al., *Data-driven state of charge estimation for lithium-ion battery packs*

based on Gaussian process regression. Energy, 2020. **205**.

19. Wang, S.L., et al., *A novel charged state prediction method of the lithium ion battery packs based on the composite equivalent modeling and improved splice Kalman filtering algorithm.* Journal of Power Sources, 2020. **471**.

20. Chen, L., et al., *Remaining useful life prediction for lithium-ion battery by combining an improved particle filter with sliding-window gray model.* Energy Reports, 2020. **6**.

21. Sun, L., G.R. Li, and F.Q. You, *Combined internal resistance and state-of-charge estimation of lithium-ion battery based on extended state observer.* Renewable & Sustainable Energy Reviews, 2020. **131**.

22. Sun, X.F., K. Zhong, and M. Han, *A hybrid prognostic strategy with unscented particle filter and optimized multiple kernel relevance vector machine for lithium-ion battery.* Measurement, 2021. **170**.

23. Zheng, C.W., Z.Q. Chen, and D.Y. Huang, *Fault diagnosis of voltage sensor and current sensor for lithium-ion battery pack using hybrid system modeling and unscented particle filter.* Energy, 2020. **191**.

24. Zhengxin, J., et al., *An Immune Genetic Extended Kalman Particle Filter approach on state of charge estimation for lithium-ion battery.* Energy, 2021. **230**.

25. Wu, M.Y., L.L. Qin, and G. Wu, *State of charge estimation of power lithium-ion battery based on an adaptive time scale dual extend Kalman filtering.* Journal of Energy Storage, 2021. **39**.

26. Zhu, Q., et al., *A state of charge estimation method for lithium-ion batteries based on fractional order adaptive extended kalman filter.* Energy, 2019. **187**.

27. Li, W.H., et al., *Electrochemical model-based state estimation for lithium-ion batteries with adaptive unscented Kalman filter.* Journal of Power Sources, 2020. **476**.

28. Ben Sassi, H., F. Errahimi, and N. ES-Sbai, *State of charge estimation by multi-innovation unscented Kalman filter for vehicular applications.* Journal of Energy Storage, 2020. **32**.

29. Yang, F.F., et al., *State-of-charge estimation of lithium-ion batteries using LSTM and UKF.* Energy, 2020. **201**.

30. Jiang, C., et al., *A state-of-charge estimation method of the power lithium-ion battery in complex conditions based on adaptive square root extended Kalman filter.* Energy, 2021. **219**.

31. Zhang, S.Z., X. Guo, and X.W. Zhang, *A novel one-way transmitted co-estimation framework for capacity and state-of-charge of lithium-ion battery based on double adaptive extended Kalman filters.* Journal of Energy Storage, 2021. **33.**

32. Zhang, K., et al., *State of Charge Estimation for Lithium Battery Based on Adaptively Weighting Cubature Particle Filter.* Ieee Access, 2019. **7**.

33. Zhou, Z.K., et al., *An efficient screening method for retired lithium -ion batteries based on support vector machine.* Journal of Cleaner Production, 2020. **267**.

34. Li, N.S., et al., *Study on the environmental adaptability of lithium-ion battery powered UAV under extreme temperature conditions.* Energy, 2021. **219**.

35. Li, C.L., et al., *Simplified electrochemical lithium-ion battery model with variable solid-phase diffusion and parameter identification over wide temperature range.* Journal of Power Sources, 2021. **497**.

36. Wu, W.X., et al., *Impact of low temperature and charge profile on the aging of lithium-ion battery: Non-invasive and post-mortem analysis.* International Journal of Heat and Mass Transfer, 2021. **170**.

37. Xuan, D.J., et al., *Real-time estimation of state-of-charge in lithium-ion batteries using improved central difference transform method.* Journal of Cleaner Production, 2020. **252**.

38. Chemali, E., et al., *State-of-charge estimation of Li-ion batteries using deep neural networks: A machine learning approach.* Journal of Power Sources, 2019. **400**.

39. Lipu, M.S.H., et al., *Extreme Learning Machine Model for State-of-Charge Estimation of Lithium-Ion Battery Using Gravitational Search Algorithm.* Ieee Transactions on Industry Applications, 2019. **55**(4).

40. Song, X.B., et al., *Combined CNN-LSTM Network for State-of-Charge Estimation of Lithium-Ion Batteries.* Ieee Access, 2019. **7**.

41. Zhu, X.Y., P. Zhang, and M. Xie, *A Joint Long Short-Term Memory and AdaBoost regression approach with application to remaining useful life estimation.* Measurement, 2021. **170**.

42. Shahraki, A., M. Abbasi, and O. Haugen, *Boosting algorithms for network intrusion detection: A comparative evaluation of Real AdaBoost, Gentle AdaBoost and Modest AdaBoost.* Engineering Applications of Artificial Intelligence, 2020. **94**.

43. Wong, L.A., et al., *Optimal placement and sizing of battery energy storage system for losses reduction using whale optimization algorithm.* Journal of Energy Storage, 2019. **26**.

44. Talaat, M., B.E. Sedhom, and A.Y. Hatata, *A new approach for integrating wave energy to the grid by an efficient control system for maximum power based on different optimization techniques.* International Journal of Electrical Power & Energy Systems, 2021. **128**.